creative commons
COMMONS DEED

저작자표시-비영리-변경금지 2.0 대한민국

이용자는 아래의 조건을 따르는 경우에 한하여 자유롭게

- 이 저작물을 복제, 배포, 전송, 전시, 공연 및 방송할 수 있습니다.

다음과 같은 조건을 따라야 합니다:

저작자표시. 귀하는 원저작자를 표시하여야 합니다.

비영리. 귀하는 이 저작물을 영리 목적으로 이용할 수 없습니다.

변경금지. 귀하는 이 저작물을 개작, 변형 또는 가공할 수 없습니다.

- 귀하는, 이 저작물의 재이용이나 배포의 경우, 이 저작물에 적용된 이용허락조건을 명확하게 나타내어야 합니다.
- 저작권자로부터 별도의 허가를 받으면 이러한 조건들은 적용되지 않습니다.

저작권법에 따른 이용자의 권리는 위의 내용에 의하여 영향을 받지 않습니다.

이것은 이용허락규약(Legal Code)을 이해하기 쉽게 요약한 것입니다.

Disclaimer

dCollection

Master's Thesis of Landscape Architecture

A multi-layer model for transpiration of urban tree considering vertical structure

수직적 구조를 고려한 도시 수목의 증산량 산정 다층 모델

August 2020

Graduate School of Seoul National University
Department of Landscape Architecture and Rural Systems Engineering, Landscape Architecture Major

Seok Hwan Yun

A multi-layer model for transpiration of urban tree considering vertical structure

Under the Direction of Adviser, Prof. Dong Kun Lee

Submitting a master's thesis of Landscape Architecture

July 2020

Graduate School of Seoul National University
Department of Landscape Architecture and Rural Systems Engineering, Landscape Architecture Major

Seok Hwan Yun

Confirming the master's thesis written by
Seok Hwan Yun
July 2020

Chair _____(Seal)
Vice Chair _____(Seal)
Examiner _____(Seal)

Abstract

As the urban heat island has been intensified, the cooling effect of urban trees is becoming important. Tree can reduce the radiant heat reaching the surface of the urban area by blocking or reflecting the radiant heat. In addition, the surface temperature of the tree is lower than that of the impervious surface such as asphalt and concrete, resulting in lower longwave radiation. Transpiration of tree also have cooling effect by releasing water into the atmosphere through the stomata of leaves, which reduces urban sensible heat by increasing latent heat. However, most previous studies which have conducted to calculate the transpiration rate have not focused on urban trees or oversimplified plant physiological process.

I propose a multi-layer model for transpiration of urban tree accounting for plant physiological process considering the vertical structure of trees and buildings. It is expanded from urban canopy model to simulate photosynthetically active radiation and leaf surface temperature accurately. To evaluate how building and tree conditions affect transpiration, I simulate transpiration by scenarios varying conditions of building height, tree location and vertical leaf area variation of trees. Simulations are conducted on four LAD distribution of trees; (1) Constant Density (C.D), (2) High Density, few layers (H.D), (3) High Density in Middle layers (M.H.D), (4) High Density in lower layers (L.H.D). LAI and tree height is same in all cases. The scenarios include three types of surrounding building (12m, 24m, and 36m) and two types of tree location (South and North). One of the

day that was a clear day, did not have rain back and forth, had high air temperature, low relative humidity is selected (1 August 2018) in Seoul (126.9658, 37.57142) to simulated, so that transpiration can occur highly.

The result show transpirative-efficient LAD distribution differs depending on tree structure and surrounding building height. The north tree surrounded by low building is most efficient for transpiration. The difference in tree transpiration during a day is up to 24.1%(south), 13.2%(north) depending on the building height. In scenario where building height are high(3H) and low(1H), the variations in tree transpiration during a day is up to 8.3% (3H) and 7.4%(1H) according to LAD distribution.

This model can be a useful tool for providing guideline on the plantation of thermo-efficient trees depending on the structure or environment of the city. And if radiant heat reduction effects are analyzed together in future studies, it will be able to get more accurate insight into the cooling effects of trees

Keyword : Urban heat island, Urban street tree, Transpiration, Multi-layer model, Urban canopy model, Cooling effect, LAD

Student Number : 2018-22915

Table of Contents

List of Figures

List of Tables

Chapter 1. Introduction

Urban heat island refers to the phenomenon in which urban area more generates and preserves heat than the surrounding area, resulting in higher temperatures, and increase the violence of urban residents, which directly and indirectly affects human health and well-being [1]. And urban heat island is becoming more serious due to urbanization and climate change [2-4].

One of the representative ways to solve the problem of heat island in cities is using the cooling effect of trees [5-11]. The cooling effects of trees can be distinguished by radiative heat reduction and transpiration [12-13]. The radiative heat reduction is that trees reduce the radiant heat reaching the surface of the urban area by blocking or reflecting the radiant heat [10,14]. It is an effective way to cool the space under the trees by generating shadows [15]. In addition, the surface temperature of the trees is lower than that of the impervious surface such as asphalt and concrete, resulting in lower longwave radiation [16]. The above-mentioned reduction of radiant heat consequently serves to lower the temperature. Second, Transpiration is the process of releasing water absorbed through roots into the atmosphere through the stomata of plant leaves [17], which reduces urban sensible heat by increasing latent heat [18]. These two actions play important roles in relieving urban heat [18-20]. While the radiant heat reduction effect of trees has been well

defined, but the transpiration effect in urban areas has not been analyzed in the previous studies.

There has been a lot of research on calculating transpiration at the canopy scale focusing rural or cropland area. In order to describe the fluxes of energy and water is necessary to provide a partition of the canopy [21]. The method to make a partition of the canopy can be summarized in three: big-leaf, two-leaf, multi-layer. Big-leaf model is simplest approach that the canopy is considered as a single leaf [22]. One of the big-leaf model, Penman-Monteith model is usually adopted to estimate potential evapotranspiration from a vegetated surface [23]. However, the surface temperature between the leaves exposed to sunlight and the leaves in the shadows varies, resulting in a difference of transpiration [24-26]. Hence least two different classes of leaves, sunlit and shaded, are necessary to calculate transpiration exactly. To reflect this, two-leaf model was developed and demonstrated that tow-leaf approach is significantly better that big-leaf models [21,27,28]. Finally, the most accurate and sophisticated model, multi-layer model, is developed, where tree is divided in multiple layer and all the quantities are estimated independently for each layer and integrated to obtain the flux at the canopy scale [29-31]. Most of the models for calculating transpiration, however, focus on forests and orchards, and research on urban trees is insufficient.

In recent years, a number of urban canopy model consider the influence of vegetation on energy and water balances; Short ground vegetation [32], trees [33-34], deciduous and evergreen shrubs and

trees [35], plant types [36]. Hence, while there are many urban canopy models that describe plants, most of them still simplify or calculate the plant physiological process in an empirical way.

In this study, I propose a multi-layer model that considers the vertical structure of trees and building to calculate the transpiration of urban trees. This model is expanded from an urban canopy model, MMRT (Multi-layer Mean Radiant Temperature) model, where the urban environment consisting of buildings and vegetation is divided into multiple layers and radiation transfer is calculated at each layer. I simulate tree transpiration by scenarios, which consider building height, tree location and vertical variation of trees. This thesis will first describe the model, set up the scenario, and calculate and compare the transpiration according to the scenarios. The results will have implications for urban cooling studies and policies using urban trees.

Chapter 2. Method

2.1. Research flow

This study focuses on developing a multi-layer model to calculate urban tree transpiration considering vertical structure of trees and building. In scenario simulation, the transpiration is simulated and compared by scenarios varying building height, tree location and leaf area density(LAD) distribution of tree. Fig. 1 presents a flow chart of our methodology.

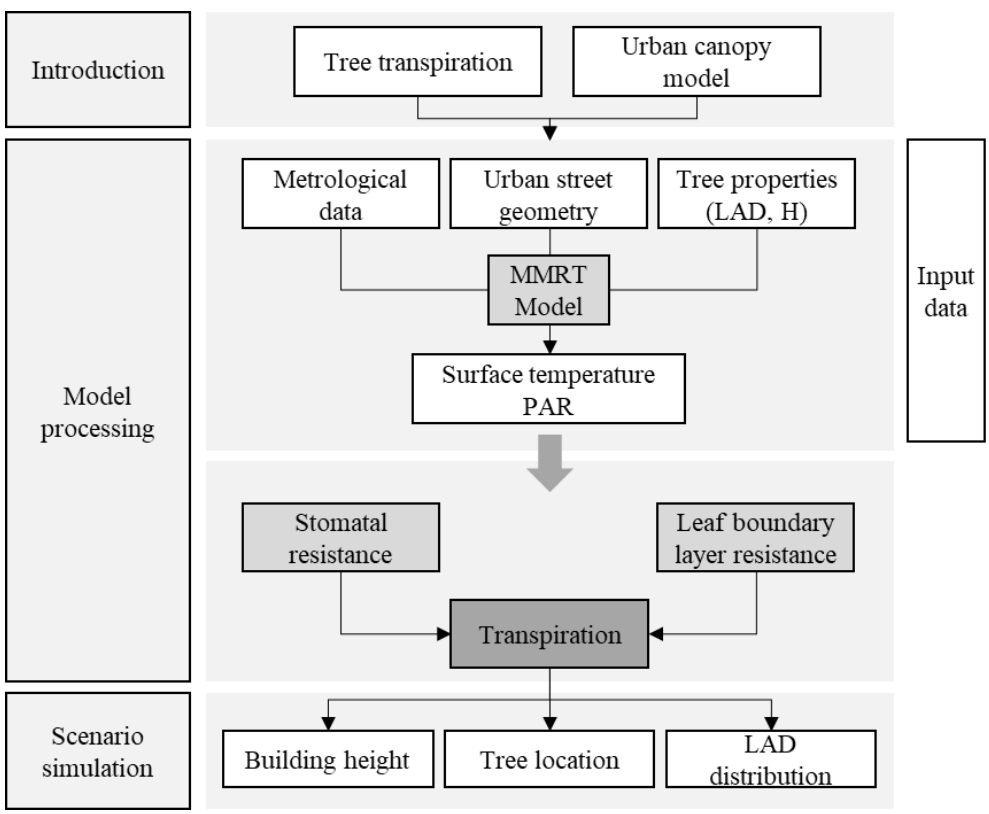

Figure 1 Research process

2.2. Model description

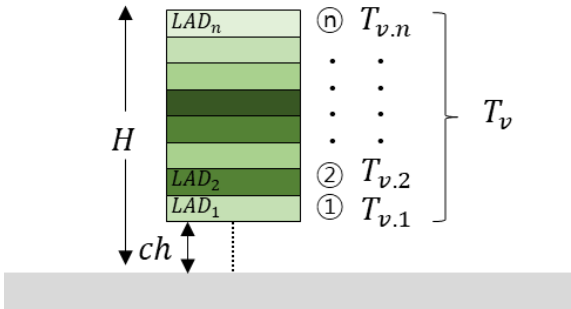

Figure 2 Model base domain

In this study, the multi-layer model reflecting the vertical structure of tree consists of n layers of crown area at intervals of 1m except for the ground level of single tree (Fig. 2). Among the variables needed to calculate the transpiration, 수목의 구조(LAD, height, crown area), leaf surface temperature through MMRT model, and canopy height are given at each layer.

2.2.1. Input data

The main input data for calculating the transpiration are meteorological data and tree properties (Table 1). Meteorological data can be obtained through the surrounding automatic weather station(AWS).

Table 1 Meteorological data, tree properties for input data

Input data	Parameter	Units
Air temperature	T_{air}	℃
Wind speed	u_a	$m\ s^{-1}$
Relative humidity	RH	%
Air pressure	P_{atm}	Pa
Cloud cover	CF	−
Leaf area index	LAI	−
Leaf area density	LAD	$m^2 m^{-3}$
Canopy height	H_c	m
Leaf width	d_{leaf}	cm

2.2.2. Model processing

The proposed model to calculate transpiration is based on Ohm's Law resistance analog equation, which is used in many leaf energy flux studies [31,37].

$$T_v = \frac{p_a(q_{sat}(T_s) - q_a)}{r_a + r_b + r_s} \quad (1)$$

where q_a $(-)$ is the specific humidity of the air at the reference height z_{atm} (m), $q_{sat}(T_s)$ $(-)$ is the specific humidity at saturation at leaf surface temperature T_s (℃), p_a (kgm^{-3}) is air density which can be calculated using the ideal gas law, expressed as a function of air

temperature T_a (℃), and atmospheric pressure P_{atm} (Pa), and r_a, r_b and r_s (sm^{-1}) are the aerodynamic resistance, leaf boundary resistance and stomatal resistance, respectively.

The specific humidity at saturation and the specific humidity of the air are calculated by Eq. (2) [38]. The air vapor pressure e_a is calculated with the saturation vapor pressure e_{sat} and relative humidity RH (%) using Eq. (3). The saturation vapor pressure is calculated using Eq. (4) from Arden−Buck equation [39−40].

$$q_a = 0.622e_a/(P_{atm} - 0.378e_a) \quad (2)$$

$$e_a = e_{sat}RH/100 \quad (3)$$

$$e_{sat} = 100 \times 6.1121exp\left(18.678 - \frac{\mathrm{T}}{234.5}\right)\left(\frac{\mathrm{T}}{257.14+\mathrm{T}}\right) \quad (4)$$

The transpiration model consists largely of calculating 1) PAR (Photosynthetically Active Radiation, μmol $m^{-2}s^{-1}$) &, Leaf surface temperature, 2) Leaf boundary layer resistance 3) Stomatal resistance.

2.2.2.1. PAR & Leaf surface temperature

One of the key part of the model is the calculation of the transpiration using PAR and leaf surface temperature each layer, which is calculated by MMRT model [34]. MMRT model simulates shortwave and longwave radiation exchanges for the view factor between each urban element, with air temperature, dew point, wind

speed, cloud cover, and relative humidity. I calculate the shortwave radiation and leaf surface temperature of each layer as MMRT model to reflect the variation in the transpiration caused by different PAR and surface temperatures depending on the location within the tree. The detailed algorithm is described in [34]. As result of MMRT model is shortwave radiation $\mathrm{SW}\ (\mathrm{Wm^{-2}})$, I multiply 4.57 to convert unit($\mu\mathrm{mol}\ \mathrm{m^{-2}s^{-1}}$, [41]) and 0.45 again because the proportion of PAR (is often defined as the 400 to 700 nm) in total solar radiation is approximately 45% [42] and many study used it [43–45].

$$\mathrm{PAR} = 4.57 \times 0.45 \times SW \quad (5)$$

2.2.2.2. Leaf boundary layer resistance

The leaf boundary layer resistance is calculated by the mean plant leaf boundary conductance $g_b\ (ms^{-1})$ using Eq. (6), which is function of wind speed and therefore of height within the canopy. I follow Eq. (7) from [46] and used by [38,47,48].

$$r_b = 1/g_b \quad (6)$$

$$g_b = a\left(u(H_k)/d_{leaf}\right)^{1/2} \quad (7)$$

where $a = 0.01\ (ms^{-1/2})$ is an empirical coefficient [47], $d_{leaf}\ (m)$ is the characteristic leaf dimension, often referred to as leaf width, and $u(H_k)\ (ms^{-1})$ is wind speed at each layer height H_k.

The wind speed profile is assumed to be logarithmic above the urban canopy, exponential with in the urban canyon using Eqs. 8−9 [49−51].

$$u_{H_c} = u_a \frac{\ln\left(\frac{H_c - d_0}{z_o}\right)}{\ln\left(\frac{z_{atm} - d_0}{z_o}\right)} \quad (8)$$

$$u_{H_k} = u_{H_c} \exp\left(-\beta\left(1 - \frac{H_k}{H_c}\right)\right) \quad (9)$$

where $u_a\ (ms^{-1})$ is the wind speed at reference height and $z_o\ (m)$ is the aerodynamic roughness length, which is calculated by Eq. (9) [49−50].

$$z_o = 0.1H_c \quad (9)$$

where $u_a\ (ms^{-1})$ is the wind speed at reference height and $\beta\ (-)$ is the light extinction parameter, which are calculated from [52]. $d_0\ (m)$ and $z_o\ (m)$ are the zero displacement height and aerodynamic roughness length, respectively, which are calculated according to the approach developed by [53] and modified by [54] as follows using Eqs. 10−11:

$$d_0 = \left(1 - \alpha_{\bar{A}}^{-\lambda^p}(\lambda^p - 1)\right) H_c \quad (10)$$

$$z_o = H_c\left(1 - \frac{d_0}{H_c}\right) \exp\left[-\left(\frac{1}{k^2} 0.5\beta_A C_{Db}\left(1 - \frac{d_0}{H_c}\right)\frac{\{A_{f,b} + P_v A_{f,v}\}}{A_{tot}}\right)^{-0.5}\right] \quad (11)$$

where $k = 0.4\ (-)$ is the von Karman constant, and $\alpha_A = 0.43\ (-)$, $\beta_A = 1\ (-)$, $C_{Db} = 1.2\ (-)$ are parameter values for staggered arrays [53]. $H_c\ (m)$ is the canopy height, $\lambda^p\ (-)$ the plan area index of the urban roughness elements, $A_{f,b}$ (m) the actual frontal area of buildings, $A_{f,v}$ (m) the actual frontal area of vegetation, $A_{tot}\ (m)$ the total urban plan area, and P_v (-) the ratio between vegetation drag C_{Dv} and building drag C_{Db}. These parameters are calculated from [51, 54-56]. For volumetric/aerodynamic porosity, light extinction parameter is calculated as [57], assuming spherical leaf angle distribution.

2.2.2.3. Aerodynamic resistance

The aerodynamic resistance is calculated by simpler method [38], which assume neutral condition as follows using Eqs. 12-13:

$$r_a = \frac{1}{k^2 u_{H_k}} \left[\frac{\ln(z_{atm} - d_0)}{z_o}\right] \left[\frac{\ln(z_{atm} - d_0)}{z_{oh}}\right] \quad (12)$$

$$z_{oh} = 0.1 z_o \quad (13)$$

where $z_{oh}\ (m)$ is the roughness length for heat.

2.2.2.4. Stomatal resistance

As reciprocal of stomatal conductance is stomatal resistance, stomatal conductance $g_s\ (\mathrm{mol\ m^{-2}s^{-1}})$ is caculated first. Many

studies reported that stomatal conductance was closely coupled with leaf photosynthesis [58−59]. In proposed model, stomatal conductance is calculated as a function of leaf photosynthesis A_n $(\mu\text{mol m}^{-2}\text{s}^{-1})$ by Eq. (14) from [60] used by [31,59,61].

$$g_s = \frac{\text{m}A_n hs}{C_s} + g_0 \quad (14)$$

where m $(-)$ is the slope, g_0 $(\text{mol m}^{-2}\text{s}^{-1})$ is the zero intercept, hs and C_s (ppm) are, respectively, relative humidity and CO2 concentration at the leaf surface. In this model, modified equation is used from [62], by using CO2 concentration C_a (ppm), relative humidity rh $(-)$ in the air as follows using Eq. (15):

$$g_s = \frac{\text{m}A_n rh}{C_a} + g_0 \quad (15)$$

The leaf photosynthesis is simulated according to [63]. The version of the model proposed by [62] was used, which is calculating photosynthesis without including the potential limitation arising from triose phosphate utilization, and is used by [37,64].

$$A_n = \left[1 - \frac{0.5O}{\tau C_i}\right] \min\left(W_c, W_j\right) - R_d \quad (16)$$

where W_c $(\mu\text{mol m}^{-2}\text{s}^{-1})$ is the carboxylation rate when ribulose bisphosphate(RuBP) is saturated, W_j $(\mu\text{mol m}^{-2}\text{s}^{-1})$ is the

carboxylation rate when RuBP regeneration is limited by electron transport, τ is the specificity factor for Rubisco [65], R_d ($\mu mol\ m^{-2}s^{-1}$) is the rate of CO_2 evolution in light that results from processes other than photorespiration, and O and C_i (Pa) are the partial pressures of O_2 and CO_2 in interior leaf, respectively. In proposed model, $C_i/C_a = 0.7$ is used, where C_a (Pa) is partial pressures of CO_2 in air, which is what is typically observed in C3 plants under favorable conditions [58,66,67].

W_c obeys competitive Michaelis–Menten kinetics with respect to CO_2 and O_2 as follows using Eq. (17):

$$W_c = \frac{V_{cmax} C_i}{C_i + K_c\left(1 + \frac{O}{K_o}\right)} \quad (17)$$

where V_{cmax} ($\mu mol\ m^{-2}s^{-1}$) is the maximum rate of carboxylation, and K_c and K_o (Pa) are Michaelis constants of Rubisco for carboxylation and oxygenation, respectively.

W_j is controlled by the rate of electron transport J ($\mu mol\ m^{-2}s^{-1}$) which depends on PAR, which are calculated as follows using Eqs. 18–19:

$$W_j = \frac{JC_i}{4\left(C_i + \frac{O}{\tau}\right)} \quad (18)$$

$$J = \frac{\alpha \times PAR}{\left(1 + \frac{\alpha^2 PAR^2}{{J_{max}}^2}\right)^{1/2}} \quad (19)$$

where J_{max} ($\mu mol\ m^{-2}s^{-1}$) is the light−saturated rate of electron transport, and α is the quantum yield that means efficiency of light energy conversion on an incident light basis.

The coefficients for V_{cmax}, J_{max}, K_c, K_o, R_d and τ are strong, non−linear functions of temperature [68−69]. One temperature function used for K_c, K_o, R_d and τ is Eq. (20) from [62]:

$$\text{Parameter}(K_c, K_o, R_d, \tau) = \exp(c - \Delta H_a / R T_{s'}) \quad (20)$$

where c ($-$) is a dimensionless, scaling constant, ΔH_a ($J\ mol^{-1}$) is an activation energy, R ($8.3143 J K^{-1} mol^{-1}$) is the gas constant and $T_{s'}$ (K) is a leaf surface temperature. The temperature dependence of V_{cmax} and J_{max} is Eq. (21) from [62,70]:

$$\text{Parameter}(V_{cmax}, J_{max}) = \frac{\exp(c - \Delta H_a / R T_{s'})}{1 + \exp[(\Delta S T_{s'} - \Delta H_d)/(R T_{s'})]} \quad (21)$$

where ΔH_d ($J\ mol^{-1}$) is an energy of deactivation and ΔS ($J K^{-1} mol^{-1}$) is an entropy term. The linear relationships commonly observed between leaf photosynthetic capacities and amount of leaf nitrogen on an area basis N_a ($g\ m^{-2}$) [62,71−73]. To account for linear relationships, the scaling factors c for V_{cmax}, J_{max}, R_d is calculated by Eq. (22) from [64].

$$c = a_N + b_N \ln(N_a) \quad (22)$$

In proposed model, the amount of leaf nitrogen is estimated from daily PAR intercepted by leaves $\mathrm{PAR_i}$ $(\mathrm{mol\ m^{-2}d^{-1}})$ by an empirical linear relationship Eq. (23) from [74].

$$N_a = \mathrm{a_{Na}} + b_{Na} PAR_i \qquad (23)$$

The stomatal resistance through stomatal conductance of Eq. (10) is expressed in biochemical units of $(\mathrm{m^2 s\ mol^{-1}})$. The conversion to common units $(\mathrm{s\ m^{-1}})$ for Eq. (1) is obtained as follows using Eq. (24) from [75]:

$$r_s(sm^{-1}) = \frac{\mathrm{T_f}\ P_{atm}}{0.0224 T_{s'}\ P_{atm,0}} r_s(\mathrm{m^2 s\ mol^{-1}}) \qquad (24)$$

where $\mathrm{T_f} = 273.15\ (K)$ is the freezing temperature and $P_{atm,0} = 101325\ (\mathrm{Pa})$ is a reference atmospheric pressure.

A complete list of the parameters for calculating resistances is given in Table 3.

2.3. Scenario simulation

I simulate PAR, leaf surface temperature and finally transpiration to evaluate and compare various scenarios including height of buildings surrounding the tree, location of tree and LAD distribution of each layer. Model parameters of MMRT model are listed in the Appendix.

The domain for simulation is presented in Fig. 4. In the domain, two building, two sidewalks, one road, two trees, and the width and height of which are denoted in domain. The tree height is 12m, tree crown width is 6m, and tree vertical layer thickness is 1m.

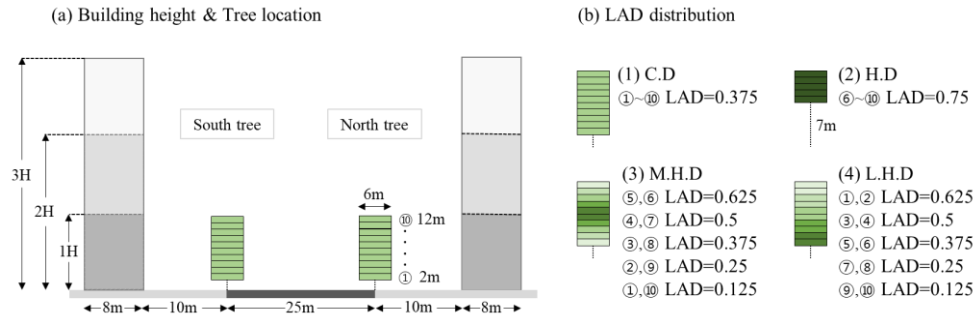

Figure 3 Domain for simulation

2.3.1. Tree location

Transpiration can be varied by tree position with building because of solar radiance absorption. To evaluate the differences depending on the location of the tree, the E−W street is set making that two trees locate northern and southern (Fig. 4a), respectively.

2.3.2. Building height

The building environment surrounding trees affect transpiration [76], for example, reflecting radiation, intercepting shortwave radiation, emitting longwave radiation and changing canopy height. The intensity of the urban heat island changes with height/width ratio [77]. To evaluate the effect of various building environment, we control building height in three cases (1H, 2H, and 3H). Case 1H is an urban canyon with 12m buildings; case 2H is an urban canyon with 24m buildings; and case 3H is an urban canyon with 36m buildings. H means tree canopy height.

2.3.3. LAD distribution

Higher LAI of tree must lead higher transpiration. LAD distribution, however, can be various cases in same LAI. We evaluate the transpiration for four vertical structure cases; (1) Constant Density (C.D), (2) High Density, few layers (H.D), (3) High Density in Middle layers (M.H.D), (4) High Density in lower layers (L.H.D). LAI and tree height is same in all cases. The crown base height of H.D case is 7m, while other cases are 2m to make same LAI (Fig. 4b)

For the simulation, I select the 213th day of the year (DOY, 1 August) in 2018 in Seoul (126.9658, 37.57142). 213 DOY was a clear day and did not have rain back and forth. It also had high air

temperature, low relative humidity that led to higher transpiration, so that I can see difference of transpiration rate with different condition. Table 2 shows the input data for the simulations. For the simulation, O (Pa), C_a (ppm) are set as 21000 and 401.91 [78], respectively. Vertical variations of RH, C_a are ignored because variations are relatively small and varies with stable condition of air [79-81].

Table 2 Meteorological data for the model simulation

LST	800	900	1000	1100	1200	1300	1400	1500	1600	1700	1800	1900	2000
Air temperature (℃)	28.2	30.3	32.4	34.3	35.8	36.8	37.9	38.7	39.3	39.4	39	37.8	36.1
Wind speed (℃)	0.5	0.8	0.7	1	1.6	1.3	2.3	2.4	2.3	2.5	2.6	3.8	3.7
Cloud fraction	0	0	0	0	0.1	0.1	0.1	0.1	0.1	0.1	0.1	0.1	0.2
Relative humidity (%)	68	59	53	45	41	39	38	38	37	39	41	47	56

Values of the main parameters and reference used in the simulation are given in Table 3. To compare transpiration of all case relatively, parameters for calculating resistances are fixed and mainly derived by [62,64]. The leaf width d_{leaf} is set as 7.5cm of Ginkgo biloba which is planted largest proportion of street tree in Seoul [82].

Table 3 Values, units and sources of the parameters for resistances

Parameter	Value	Unit	Source
d_{leaf}	0.75	m	[84]
m	9.5	–	[31]
g_0	0.081	mol $m^{-2}s^{-1}$	H92
a_{Na}	0.46	g m^{-2}	L99b
b_{Na}	0.141	–	L99b
α	0.22	mol mol^{-1}	[31]
a_{N_Vcmax}	47.42	–	L99a
b_{N_Vcmax}	1.118	g^{-1}	L99a
a_{N_Jmax}	36.11	–	L99a
b_{N_Jmax}	0.993	g^{-1}	L99a
a_{N_Rd}	-32.85	–	L99a
b_{N_Rd}	-1.027	g^{-1}	L99a
$c(K_c)$	35.79	–	H92
$c(K_o)$	9.59	–	H92
$c(\tau)$	-3.9489	–	H92
$\Delta H_a(K_c)$	80.47×10^3	J mol^{-1}	H92
$\Delta H_a(K_o)$	14.51×10^3	J mol^{-1}	H92
$\Delta H_a(\tau)$	-28.99×10^3	J mol^{-1}	H92
$\Delta H_a(R_d)$	84.45×10^3	J mol^{-1}	H92
$\Delta H_a(V_{cmax})$	109.5×10^3	J mol^{-1}	L99a
$\Delta H_a(J_{max})$	79.5×10^3	J mol^{-1}	H92
$\Delta H_d(V_{cmax})$	199.5×10^3	J mol^{-1}	L99a
$\Delta H_d(J_{max})$	201×10^3	J mol^{-1}	H92
$\Delta S(V_{cmax})$	650	J $K^{-1}mol^{-1}$	H92
$\Delta S(J_{max})$	650	J $K^{-1}mol^{-1}$	H92

Sources: H92=[62], L99a=[64], L99b=[74].

Chapter 3. Results and Discussion

3.1. Parameter

3.1.1. PAR & leaf surface temperature

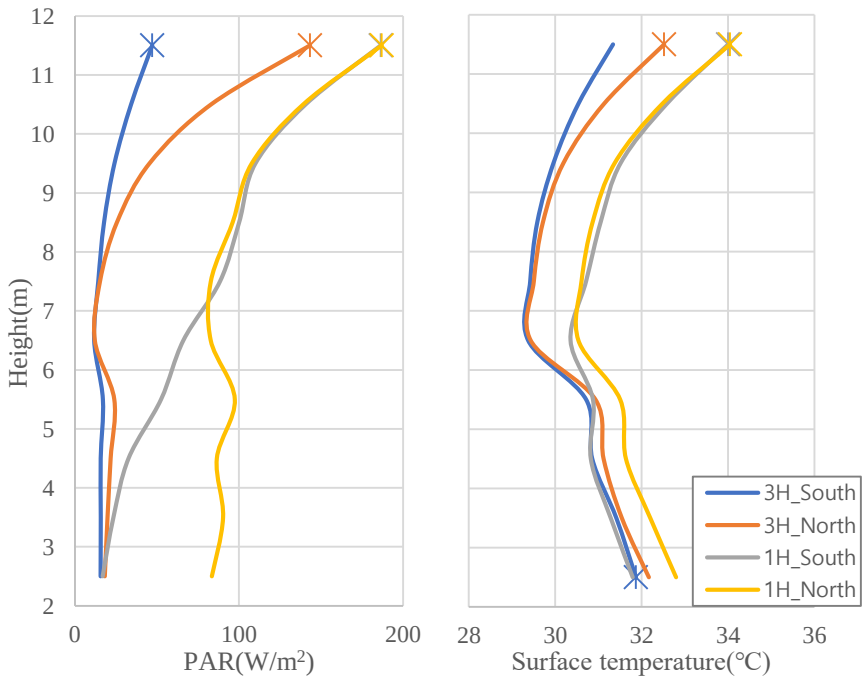

Figure 4 Vertical profile of PAR(left) and leaf surface temperature(right) according to tree location(south, north) / building height(1H,3H). (LAD distribution: C.D, time: 15h and *: maximum value, 38.7 2.4 0.1 37)

The results of PAR and leaf surface temperature simulated by MMRT model are shown in Fig. 4. When the building is low(1H), higher PAR and surface temperature are resulted. PAR shows decreasing shape depending on the height, but the vertical profile of surface temperature is not. The highest surface temperature usually is in the upper layer, but the lower layer close to the ground is upper

than the middle layer due to high longwave radiation emitted from ground. This is similar to higher results as the surface temperature of the tree trunk nears the surface [77]. The pattern is obvious in the 3H, South tree, where solar radiation is largely intercepted by the building, resulting in small difference between high layer and low layer. This pattern makes a different vertical profile of surface temperature, which is slightly higher at first layer than top layer.

3.1.2. Resistances

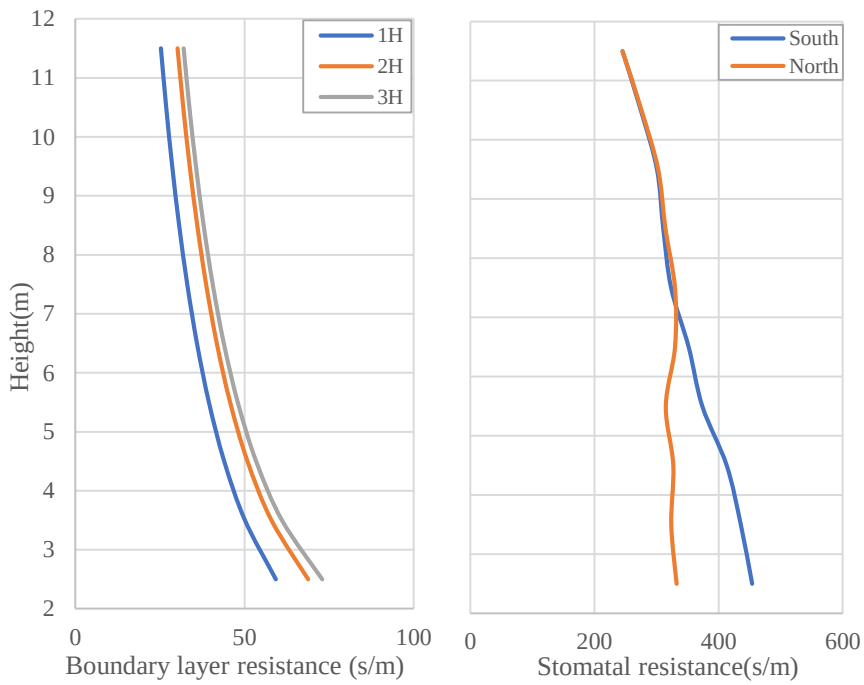

Figure 5 Vertical profile of leaf boundary layer resistance(left) and stomatal resistance(right) according to building height(1H, 2H, 3H, north tree), tree location(south, north, 1H), respectively. (LAD distribution: C.D, time: 15h)

Data in Fig. 5 show vertical profiles of leaf boundary layer resistance

and stomatal resistance. In the upper layer, it is showed relatively high wind speed and PAR, resulting in lower both resistance. In scenario of 3H, as the height decreases, the wind speed decreases significantly due to high canopy height, resulting in a large difference in boundary layer resistance.

3.2. Transpiration

3.2.1. Temporal variation

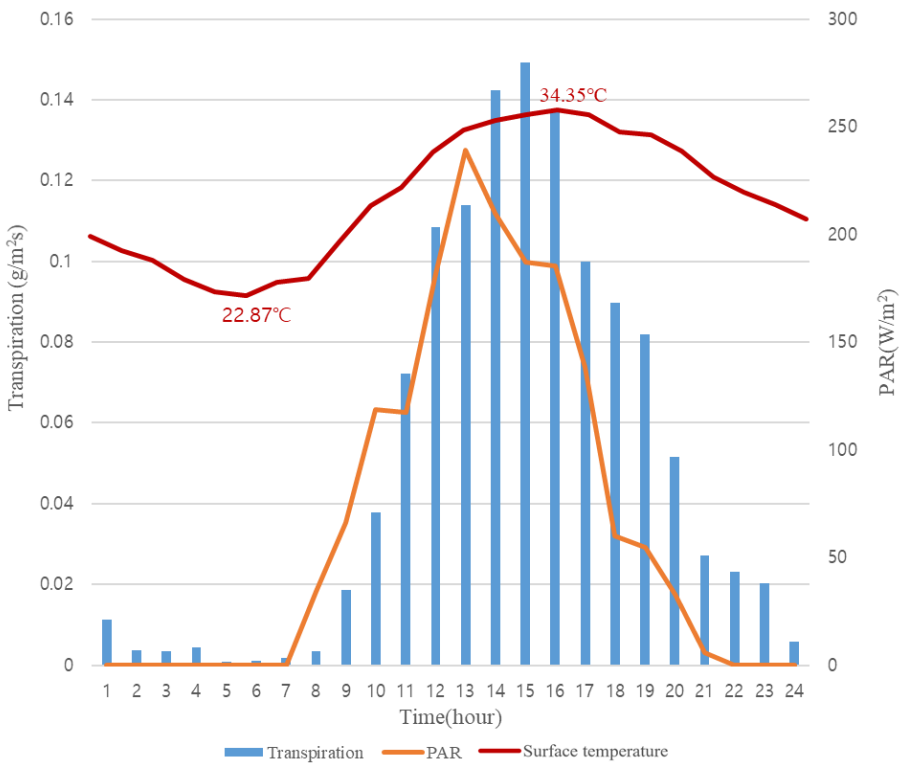

Figure 6 Temporal variation of tree transpiration rate(bar) with PAR(orange line) and surface temperature(red line) of top layer (building height: 1H, tree location: north, LAD distribution: C.D)

Fig. 6 show the result of hourly transpiration rate of tree along

with PAR and leaf surface temperature. Despite the highest PAR causing the lowest stomatal resistance, it does not show the highest result transpiration rate at the time with highest PAR. This is because the temporal pattern of leaf surface temperature, another factor that has a dominant effect on transpiration, does not perfectly match PAR pattern. Therefore, transpiration rate is high at the time that the surface temperature and PAR are simultaneously high.

3.2.2. Scenarios simulation

(a)

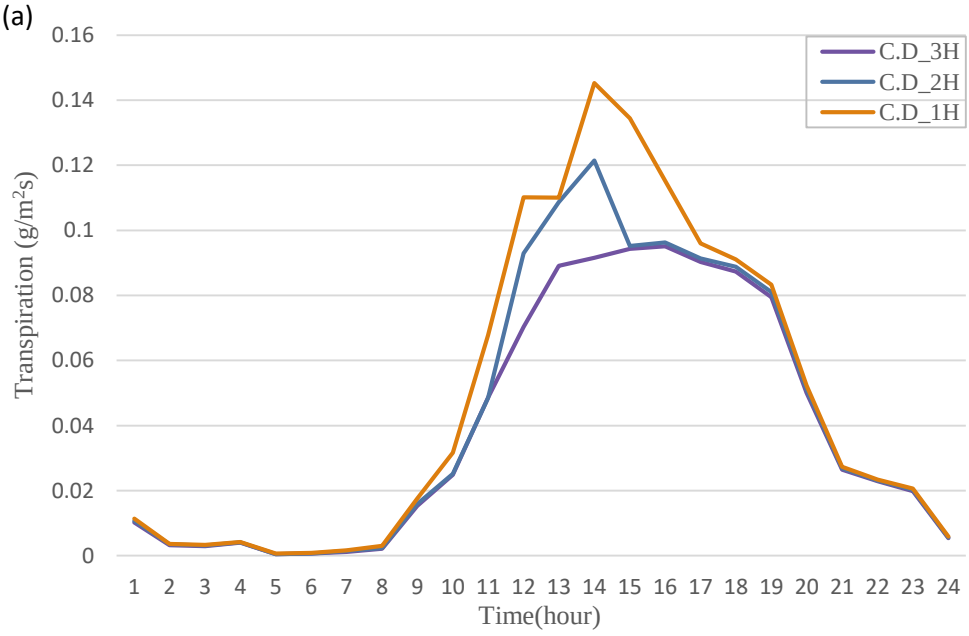

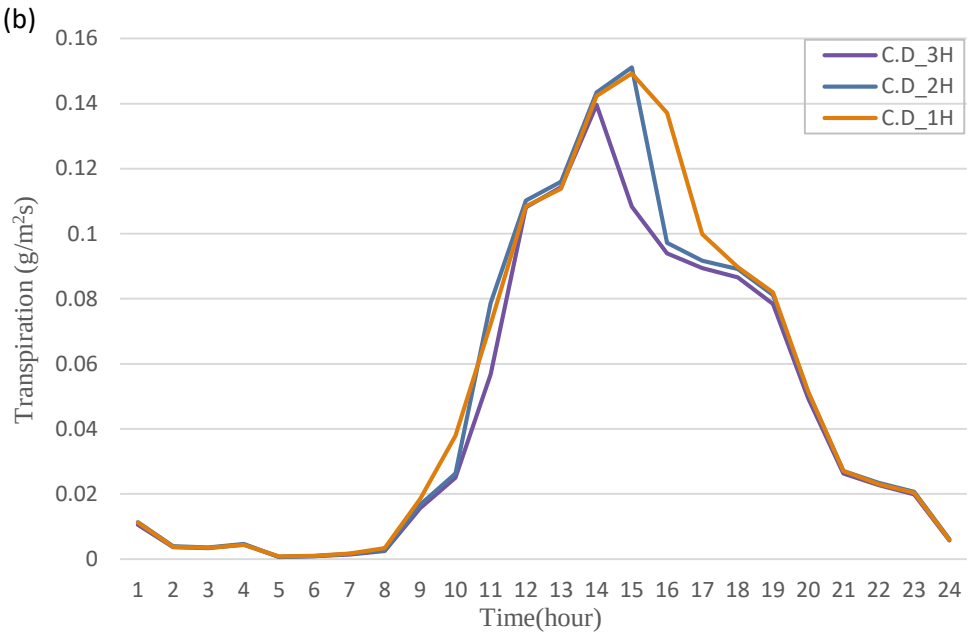

Figure 7 Transpiration rate changes by the building height scenarios during a day (1H, 2H, 3H). (a) South tree (b) North tree. (LAD distribution: C.D)

In all of the tree location scenarios, the lower height of the surrounding buildings, the higher the transpiration rate (Fig. 7). The difference of transpiration rate mainly occurs at the time daytime. However, the variation of south tree is higher than north tree according to building height. In the C.D LAD distribution scenarios, the difference in tree transpiration during a day is up to 24.1%(south), 13.2%(north) depending on the building height (Fig. 7). The south tree is more sensitive to the height of the building because it is close to the building that forms the shadow.

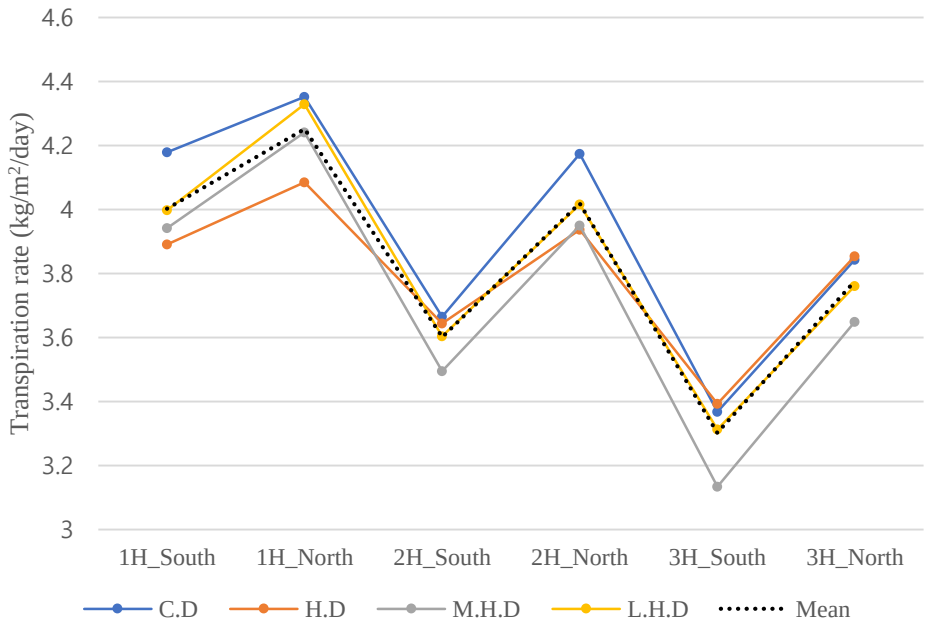

Figure 8 Transpiration rate changes by LAD distribution, tree location, building height scenarios

Fig. 8 shows the total transpiration rate during the day according to all scenarios for four LAD distributions, two tree locations and three building heights. Depending on the scenarios, the LAD distribution of the most evaporating trees differed, which means that the most efficient/inefficient trees vary depending on urban space and the arrangement of trees. In particular, it is noteworthy that the H.D. case, which has high LAD density, results in most efficiency at 3H scenarios and worst efficiency at 1H scenarios, regardless of tree location.

Fig. 8 shows that the LAD distribution of trees is relatively important in environment with high building. In scenario where building height are high(3H), the variations in tree transpiration

during a day is up to 8.3%(south) and 5.6%(north) according to LAD distribution. In scenario of 1H, the variations are 7.4%(south) and 6.5%(north). In addition, the difference between north and south trees is greater if the building is high compared low (14.4% in 3H, 6.2% in 1H).

The results of scenario simulation suggest that the location and shape of trees that are efficient for cooling, vary depending on the urban environment. This model can better evaluate the cooling effect of trees by considering the radiant heat intercepting effect of trees. For example, the shallow canyon can be hotter due to high exposure of the canyon's surfaces to the intense solar radiation [77,84]. And the air temperature with taller buildings are lower due to their shading effect [85]. Therefore, in consideration of that the shallow street canyon need higher cooling effect, the tree which have big crown could be effective in terms of both of transpiration and shading [86-87]. The results can be used to design street tree for improved thermal comfort when used with air temperature, humidity, and wind speed.

3.3. Model limitations and future development

This study proposes a multi-layer model that considers the vertical structure of trees and building to calculate the transpiration rate of urban trees. That generates difference between the vapor pressure deficit, wind speed, and resistance values, which makes in

turn difference result of transpiration depending on the scenarios. Although many parameters which can lead to restrictive result are fixed to simulate transpiration, it is meaningful to compare the relative transpiration rate of each scenarios. Future studies need to estimate and verify parameters of model to improve accuracy.

And the MMRT model would calculate the surface temperature higher than it actually is because it has limitations in processing latent heat, making the latent heat very small by using a very large Bowen ratio. Thus, in order to increase accuracy, this limit could be developed through feedback that calculates latent heat using transpiration of proposed model and calculates surface temperature again.

This study only dealt with the transpiration of tree cooling effects. Considering the radiative heat reduction of tree in the future, it will be a more accurate assessment of the cooling effect of trees. Under various conditions, there will be different cooling requirements, along with other thermal environments, and the shadow effects will vary significantly.

The model used only one day of weather conditions which can lead to only one case. If I simulate on days with low temperatures and high humidity, the difference may be small in each case.

Chapter 4. Conclusion

I propose a multi-layer model for calculating transpiration of urban trees. The advantage of the model is that it simulates transpiration considering the vertical structure of trees and building. To reflect vertical structure effectively, PAR and leaf surface temperature data simulated by MMRT model, one of the urban canopy model. The proposed model includes a detailed representation of plant biophysical and echophysiological characteristics.

Simulations are conducted on four LAD distribution of trees with three types of building (12m, 24m, and 36m) and two types of tree location (South and North). North tree surrounded by low building is most efficient for transpiration. The difference in tree transpiration during a day is up to 24.1%(south), 13.2%(north) depending on the building height. In scenario where building height are high(3H) and low(1H), the variations in tree transpiration during a day is up to 8.3% (3H) and 7.4%(1H) according to LAD distribution. It is similar respect to tree location.

The scenario simulation suggests that the location and shape of trees that are efficient for cooling effect, vary depending on the urban environment. This model is useful tool providing guideline on the plantation of thermo-efficient trees depending on the structure or environment of the city If I analyze transpiration and radiant heat reduction effects together in future studies, it will be able to gain more accurate insight into the cooling effects of trees.

Bibliography

[1] J. O'Loughlin, F.D.W. Witmer, A.M. Linke, A. Laing, A. Gettelman, J. Dudhia, Climate variability and conflict risk in East Africa, 1990–2009, Proc. Natl. Acad. Sci. U. S. A. 109 (2012) 18344–18349. https://doi.org/10.1073/pnas.1205130109.

[2] P. Hoffmann, O. Krueger, K.H. Schlünzen, A statistical model for the urban heat island and its application to a climate change scenario, Int. J. Climatol. 32 (2012) 1238–1248. https://doi.org/10.1002/joc.2348.

[3] D.E. Parker, Urban heat island effects on estimates of observed climate change, Wiley Interdiscip. Rev. Clim. Chang. 1 (2010) 123–133. https://doi.org/10.1002/wcc.21.

[4] H. Radhi, F. Fikry, S. Sharples, Impacts of urbanisation on the thermal behaviour of new built up environments: A scoping study of the urban heat island in Bahrain, Landsc. Urban Plan. 113 (2013) 47–61. https://doi.org/10.1016/j.landurbplan.2013.01.013.

[5] D. Armson, P. Stringer, A.R. Ennos, The effect of tree shade and grass on surface and globe temperatures in an urban area, Urban For. Urban Green. 11 (2012) 245–255. https://doi.org/10.1016/j.ufug.2012.05.002.

[6] A.H. Block, S.J. Livesley, N.S.G. Williams, Responding to the Urban Heat Island : A Review of the Potential of Green Infrastructure, Vic. Cent. Clim. Chang. Adapt. (2012) 1–62. http://staging.202020vision.com.au/media/1026/responding-to-the-urban-heat-island-a-review-of-the-potential-of-green-infrastructure.pdf.

[7] K.R. Gunawardena, M.J. Wells, T. Kershaw, Utilising green and bluespace to mitigate urban heat island intensity, Sci. Total Environ. 584–585 (2017) 1040–1055. https://doi.org/10.1016/j.scitotenv.2017.01.158.

[8] J. Konarska, F. Lindberg, A. Larsson, S. Thorsson, B. Holmer, Transmissivity of solar radiation through crowns of single urban trees—application for outdoor thermal comfort modelling, Theor. Appl. Climatol. 117 (2014) 363–376. https://doi.org/10.1007/s00704-013-1000-3.

[9] J. Konarska, J. Uddling, B. Holmer, M. Lutz, F. Lindberg, H. Pleijel, S. Thorsson, Transpiration of urban trees and its cooling effect in a high latitude city, Int. J. Biometeorol. 60 (2016) 159–172. https://doi.org/10.1007/s00484-015-1014-x.

[10] Z. Tan, K.K.L. Lau, E. Ng, Urban tree design approaches for mitigating daytime urban heat island effects in a high-density urban environment, Energy Build. 114 (2016) 265–274. https://doi.org/10.1016/j.enbuild.2015.06.031.

[11] Y. Wang, H. Akbari, The effects of street tree planting on Urban Heat Island mitigation in Montreal, Sustain. Cities Soc. 27 (2016) 122–128. https://doi.org/10.1016/j.scs.2016.04.013.

[12] P.A. Mirzaei, F. Haghighat, Approaches to study Urban Heat Island – Abilities and limitations, Build. Environ. 45 (2010) 2192–2201. https://doi.org/10.1016/j.buildenv.2010.04.001.

[13] M.A. Rahman, A. Moser, A. Gold, T. Rötzer, S. Pauleit, Vertical air temperature gradients under the shade of two contrasting urban tree species during different types of summer days, Sci. Total Environ. 633 (2018) 100–111.

https://doi.org/10.1016/j.scitotenv.2018.03.168.

[14] H. Akbari, Shade trees reduce building energy use and CO2 emissions from power plants, Environ. Pollut. 116 (2002) 119–126. https://doi.org/10.1016/S0269-7491(01)00264-0.

[15] B.S. Lin, Y.J. Lin, Cooling effect of shade trees with different characteristics in a subtropical urban park, HortScience. 45 (2010) 83–86. https://doi.org/10.21273/hortsci.45.1.83.

[16] H. Taha, Urban climates and heat islands: Albedo, evapotranspiration, and anthropogenic heat, Energy Build. 25 (1997) 99–103. https://doi.org/10.1016/s0378-7788(96)00999-1.

[17] C. Campillo, R. Fortes, M. del Henar Prieto, Solar Radiation Effect on Crop Production, Sol. Radiat. (2012). https://doi.org/10.5772/34796.

[18] M. Ballinas, V.L. Barradas, The Urban Tree as a Tool to Mitigate the Urban Heat Island in Mexico City: A Simple Phenomenological Model, J. Environ. Qual. 45 (2016) 157–166. https://doi.org/10.2134/jeq2015.01.0056.

[19] Y. Wang, H. Akbari, The effects of street tree planting on Urban Heat Island mitigation in Montreal, Sustain. Cities Soc. 27 (2016) 122–128. https://doi.org/10.1016/j.scs.2016.04.013.

[20] G. Kim, P. Coseo, Urban park systems to support sustainability: The role of urban park systems in hot arid urban climates, Forests. 9 (2018) 1–16. https://doi.org/10.3390/f9070439.

[21] Y. Dai, R.E. Dickinson, Y.P. Wang, A two-big-leaf model for canopy temperature, photosynthesis, and stomatal

conductance, J. Clim. 17 (2004) 2281–2299. https://doi.org/10.1175/1520-0442(2004)017<2281:ATMFCT>2.0.CO;2.

[22] J.L. Monteith, Solar Radiation and Productivity in Tropical Ecosystems, J. Appl. Ecol. 9 (1972) 747. https://doi.org/10.2307/2401901.

[23] T.A. McMahon, M.C. Peel, L. Lowe, R. Srikanthan, T.R. McVicar, Estimating actual, potential, reference crop and pan evaporation using standard meteorological data: A pragmatic synthesis, Hydrol. Earth Syst. Sci. 17 (2013) 1331–1363. https://doi.org/10.5194/hess-17-1331-2013.

[24] P.S. Nobel, Photosynthetic Rates of Sun versus Shade Leaves of Hyptis emoryi Torr. , Plant Physiol. 58 (1976) 218–223. https://doi.org/10.1104/pp.58.2.218.

[25] T.L. Pons, W. Jordi, D. Kuiper, Acclimation of plants to light gradients in leaf canopies: Evidence for a possible role for cytokinins transported in the transpiration stream, J. Exp. Bot. 52 (2001) 1563–1574. https://doi.org/10.1093/jexbot/52.360.1563.

[26] M. Saudreau, A. Ezanic, B. Adam, R. Caillon, P. Walser, S. Pincebourde, Temperature heterogeneity over leaf surfaces: the contribution of the lamina microtopography, Plant Cell Environ. 40 (2017) 2174–2188. https://doi.org/10.1111/pce.13026.

[27] T.R. Sinclair, C.E. Murphy, K.R. Knoerr, Development and Evaluation of Simplified Models for Simulating Canopy Photosynthesis and Transpiration, Br. Ecol. Soc. 13 (1976) 813–829. https://www.jstor.org/stable/2402257.

[28] Y.P. Wang, R. Leuning, A two-leaf model for canopy

conductance, photosynthesis and partitioning of available energy I: Model description and comparison with a multi-layered model, Agric. For. Meteorol. 91 (1998) 89–111. https://doi.org/10.1016/S0168-1923(98)00061-6.

[29] [1] R. LEUNING, A critical appraisal of a combined stomatal-photosynthesis model for C3 plants, Plant. Cell Environ. 18 (1995) 339–355. https://doi.org/10.1111/j.1365-3040.1995.tb00370.x.

[30] R.D. Pyles, B.C. Weare, K.T. Pawu, The UCD advanced canopy- atmosphere-soil algorithm: Comparisons with observations from different climate and vegetation regimes, Q. J. R. Meteorol. Soc. 126 (2000) 2951–2980. https://doi.org/10.1256/smsqj.56916.

[31] D.D. Baldocchi, K.B. Wilson, L. Gu, How the environment, canopy structure and canopy physiological functioning influence carbon, water and energy fluxes of a temperate broad-leaved deciduous forest - An assessment with the biophysical model CANOAK, Tree Physiol. 22 (2002) 1065–1077. https://doi.org/10.1093/treephys/22.15-16.1065.

[32] Z.H. Wang, E. Bou-Zeid, J.A. Smith, A coupled energy transport and hydrological model for urban canopies evaluated using a wireless sensor network, Q. J. R. Meteorol. Soc. 139 (2013) 1643–1657. https://doi.org/10.1002/qj.2032.

[33] Y.H. Ryu, E. Bou-Zeid, Z.H. Wang, J.A. Smith, Realistic Representation of Trees in an Urban Canopy Model, Boundary-Layer Meteorol. 159 (2016) 193–220. https://doi.org/10.1007/s10546-015-0120-y.

[34] C.Y. Park, D.K. Lee, E.S. Krayenhoff, H.K. Heo, S. Ahn, T. Asawa, A. Murakami, H.G. Kim, A multilayer mean radiant

temperature model for pedestrians in a street canyon with trees, Build. Environ. 141 (2018) 298–309. https://doi.org/10.1016/j.buildenv.2018.05.058.

[35] H.C. Ward, S. Kotthaus, L. Järvi, C.S.B. Grimmond, Surface Urban Energy and Water Balance Scheme (SUEWS): Development and evaluation at two UK sites, Urban Clim. 18 (2016) 1–32. https://doi.org/10.1016/j.uclim.2016.05.001.

[36] K.A. Nice, A.M. Coutts, N.J. Tapper, Development of the VTUF−3D v1.0 urban micro−climate model to support assessment of urban vegetation influences on human thermal comfort, Urban Clim. 24 (2018) 1052–1076. https://doi.org/10.1016/j.uclim.2017.12.008.

[37] H. Sinoquet, X. Le Roux, B. Adam, T. Ameglio, F.A. Daudet, RATP: A model for simulating the spatial distribution of radiation absorption, transpiration and photosynthesis within canopies: Application to an isolated tree crown, Plant, Cell Environ. 24 (2001) 395–406. https://doi.org/10.1046/j.1365−3040.2001.00694.x.

[38] S. Fatichi, The modeling of hydrological cycle and its interaction with vegetation in the framework of climate change, Univ. Firenze. (2010) 463.

[39] A.L. Buck, New equations for computing vapour pressure and enhancement factor., J. Appl. Meteorol. 20 (1981) 1527–1532. https://doi.org/10.1175/1520−0450(1981)0202.0.CO;2.

[40] Buck Research Instruments, Humidity conversion equations, Model CR−1A Hygrom. with Autofill, Oper. Man. (2012) 20–21. http://www.hygrometers.com/wp−content/uploads/CR−1A−users−manual−2009−12.pdf.

[41] J.C. Sager, J.C.M. Farlane, Chapter 1. Radiation, Growth Chamb. Handb. 46 (2003) 30–33. https://doi.org/http://doi.acm.org/10.1145/636772.636794.

[42] W. Larcher, 1995. Physiological plant ecology, 3rd Edn. Springer− Verlag, Heidelberg, 506 p

[43] T.L. Ginter, Shade Adaptive Responses of Plants, Texas Tech U Diversity, 2001.

[44] S. Smolander, P. Stenberg, A method for estimating light interception by a conifer shoot, Tree Physiol. 21 (2001) 797–803. https://doi.org/10.1093/treephys/21.12−13.797.

[45] M. He, J.S. Kimball, M.P. Maneta, B.D. Maxwell, A. Moreno, S. Beguería, X. Wu, Regional crop gross primary productivity and yield estimation using fused landsat−MODIS data, Remote Sens. 10 (2018). https://doi.org/10.3390/rs10030372.

[46] H.G. Jones, Plants and Microclimate, Cambridge University Press, New York.

[47] B.J. Choudhury, J.L. Monteith, A four-layer model for the heat budget of homogeneous land surfaces, Q. J. R. Meteorol. Soc. 114 (1988) 373–398. https://doi.org/10.1002/qj.49711448006.

[48] W.J. Shuttleworth, R.J. Gurney, The theoretical relationship between foliage temperature and canopy resistance in sparse crops, Q. J. R. Meteorol. Soc. 116 (1990) 497–519. https://doi.org/10.1002/qj.49711649213.

[49] V. Masson, A physically−based scheme for the urban energy budget in atmospheric models, Boundary−Layer Meteorol. 94 (2000) 357–397. https://doi.org/10.1023/A:1002463829265.

[50] V. Mahat, D.G. Tarboton, N.P. Molotch, Testing above− and

below-canopy representations of turbulent fluxes in an energy balance snowmelt model, Water Resour. Res. 49 (2013) 1107–1122. https://doi.org/10.1002/wrcr.20073.

[51] N. Meili, G. Manoli, P. Burlando, E. Bou-Zeid, W.T.L. Chow, A.M. Coutts, E. Daly, K.A. Nice, M. Roth, N.J. Tapper, E. Velasco, E.R. Vivoni, S. Fatichi, An urban ecohydrological model to quantify the effect of vegetation on urban climate and hydrology (UT&C v1.0), Geosci. Model Dev. 13 (2020) 335–362. https://doi.org/10.5194/gmd-13-335-2020.

[52] J.L. Wright, Evaluating turbulent transfer aerodynamically within the microclimate of a cornfield, Univ. Cornell. (1965) 174.

[53] R.W. Macdonald, R.F. Griffiths, D.J. Hall, An improved method for the estimation of surface roughness of obstacle arrays, Atmos. Environ. 32 (1998) 1857–1864. https://doi.org/10.1016/S1352-2310(97)00403-2.

[54] C.W. Kent, S. Grimmond, D. Gatey, Aerodynamic roughness parameters in cities: Inclusion of vegetation, J. Wind Eng. Ind. Aerodyn. 169 (2017) 168–176. https://doi.org/10.1016/j.jweia.2017.07.016.

[55] G. De-xin, Z. Ting-yao, H. Shi-jie, Wind tunnel experiment of drag of isolated tree models in surface boundary layer, J. For. Res. 11 (2000) 156–160. https://doi.org/10.1007/BF02855516.

[56] D. Guan, Y. Zhang, T. Zhu, A wind-tunnel study of windbreak drag, Agric. For. Meteorol. 118 (2003) 75–84. https://doi.org/10.1016/S0168-1923(03)00069-8.

[57] Y. Dai, R.E. Dickinson, Y.-P. Wang, A Two-Big-Leaf Model

for Canopy Temperature, Photosynthesis, and Stomatal Conductance, J. Clim. 17 (2004) 2281–2299. https://doi.org/10.1175/1520-0442(2004)017<2281:ATMFCT>2.0.CO;2.

[58] S.C. Wong, I.R. Cowan, G.D. Farquhar, Stomatal conductance correlates with photosynthetic capacity, Nature. 282 (1979) 424–426. https://doi.org/10.1038/282424a0.

[59] G.J. Collatz, J.T. Ball, C. Grivet, J.A. Berry, Physiological and environmental regulation of stomatal conductance, photosynthesis and transpiration: a model that includes a laminar boundary layer, Agric. For. Meteorol. 54 (1991) 107–136. https://doi.org/10.1016/0168-1923(91)90002-8.

[60] J.T. Ball, J.A. Berry, An analysis and concise description of stomatal responses to multiple environmental factors. Planta, in press.

[61] D. Baldocchi, T. Meyers, On using eco-physiological, micrometeorological and biogeochemical theory to evaluate carbon dioxide, water vapor and trace gas fluxes over vegetation: A perspective, Agric. For. Meteorol. 90 (1998) 1–25. https://doi.org/10.1016/S0168-1923(97)00072-5.

[62] P.C. HARLEY, R.B. THOMAS, J.F. REYNOLDS, B.R. STRAIN, Modelling photosynthesis of cotton grown in elevated CO2, Plant. Cell Environ. 15 (1992) 271–282. https://doi.org/10.1111/j.1365-3040.1992.tb00974.x.

[63] G.D. Farquhar, S. von Caemmerer, J.A. Berry, A biochemical model of photosynthetic CO2 assimilation in leaves of C3 species, Planta. 149 (1980) 78–90. https://doi.org/10.1007/BF00386231.

[64] X. Le Roux, S. Grand, E. Dreyer, Franç. alain Daudet,

Parameterization and testing of a biochemically based photosynthesis model for walnut (Juglans regia) trees and seedlings, Tree Physiol. 19 (1999) 481–492. https://doi.org/10.1093/treephys/19.8.481.

[65] D.B. Jordan, W.L. Ogren, The CO 2 /O 2 specificity of ribulose 1,5−bisphosphate carboxylase/oxygenase − Dependence on ribulosebisphosphate concentration, pH and temperature, Planta. 161 (1984) 308–313. https://doi.org/10.1007/BF00398720.

[66] A.M. Hetherington, F. l. Woodward, The role of stomata in sensing and driving environmental change, Nature. 424 (2003) 528–539. https://doi.org/10.4135/9781446201091.n40.

[67] I.C. Prentice, N. Dong, S.M. Gleason, V. Maire, I.J. Wright, Balancing the costs of carbon gain and water transport: Testing a new theoretical framework for plant functional ecology, Ecol. Lett. 17 (2014) 82–91. https://doi.org/10.1111/ele.12211.

[68] I.R. JOHNSON, J.H.M. THORNLEY, Temperature Dependence of Plant and Crop Process, Ann. Bot. 55 (1985) 1–24. https://doi.org/10.1093/oxfordjournals.aob.a086868.

[69] P.C. Harley, J.D. Tenhunen, Modeling the photosynthetic response of C3 leaves to environmental factors. Modeling Photosynthesis—From Biochemistry to Canopy. Am. Soc. Agronomy. Madison (1991) 17–39. https://doi.org/10.2135/cssaspecpub19.c2

[70] F. Johnson, H. Eyring, R. Williams, The nature of enzyme inhibitions in bacterial luminescence: Sulfanilamide, urethane, temperature and pressure, Jotirnal Cell Cotnparative Physiol.

20 (1942) 247–268. https://doi.org/https://doi.org/10.1002/jcp.1030200302.

[71] C. Field, Allocating leaf nitrogen for the maximization of carbon gain: Leaf age as a control on the allocation program, Oecologia. 56 (1983) 341–347. https://doi.org/10.1007/BF00379710.

[72] J.R. Evans, Photosynthesis and nitrogen relationships in leaves of C3 plants, Oecologia. 78 (1989) 9–19. https://doi.org/10.1007/BF00377192.

[73] R. Leuning, Y.P. Wang, R.N. Cromer, Model simulations of spatial distributions and daily totals of photosynthesis in Eucalyptus grandis canopies, Oecologia. 88 (1991) 494–503. https://doi.org/10.1007/BF00317711.

[74] X. Le Roux, H. Sinoquet, M. Vandame, Spatial distribution of leaf dry weight per area and leaf nitrogen concentration in relation to local radiation regime within an isolated tree crown, Tree Physiol. 19 (1999) 181–188. https://doi.org/10.1093/treephys/19.3.181.

[75] P.J. Sellers, D.A. Randall, G.J. Collatz, J.A. Berry, C.B. Field, D.A. Dazlich, C. Zhang, G.D. Collelo, L. Bounoua, A revised land surface parameterization (SiB2) for atmospheric GCMs. Part I: Model formulation, J. Clim. 9 (1996) 676–705. https://doi.org/10.1175/1520-0442(1996)009<0676:ARLSPF>2.0.CO;2.

[76] C.P. Loughner, D.J. Allen, D.L. Zhang, K.E. Pickering, R.R. Dickerson, L. Landry, Roles of urban tree canopy and buildings in urban heat island effects: Parameterization and preliminary results, J. Appl. Meteorol. Climatol. 51 (2012) 1775–1793. https://doi.org/10.1175/JAMC-D-11-0228.1.

[77] M.A. Bakarman, J.D. Chang, The Influence of Height/width Ratio on Urban Heat Island in Hot–arid Climates, Procedia Eng. 118 (2015) 101–108. https://doi.org/10.1016/j.proeng.2015.08.408.

[78] C. Park, S. Jeong, H. Park, J. Yun, J. Liu, Evaluation of the Potential Use of Satellite–Derived XCO2 in Detecting CO2 Enhancement in Megacities with Limited Ground Observations: A Case Study in Seoul Using Orbiting Carbon Observatory–2, Asia–Pacific J. Atmos. Sci. (2020). https://doi.org/10.1007/s13143–020–00202–5.

[79] T. Brys, Z. Caputa, J. Wibig, K. Brys, K. Fortuniak, Humidity gradients in urban environments on the example of Wroclaw, Sosnowiec and Lodz. In: Kłysik K., Oke T.R., Fortuniak K., Grimmond C.S.B. & Wibig J. (eds): Fifth International Conference on Urban Climate, 1–5 September, Proceedings. 1 (2003) 41–45. http://meteo.geo.uni.lodz.pl/kf/publikacje_kf_PDF/r2003_ICUC5_Brys_etal.pdf.

[80] R. Moriwaki, M. Kanda, Vertical profiles of carbon dioxide, temperature, and water vapor within and above a suburban canopy layer in winter, 86th AMS Annu. Meet, 2006.

[81] R. Vogt, A. Christen, M.W. Rotach, M. Roth, A.N.V. Satyanarayana, Temporal dynamics of CO2 fluxes and profiles over a Central European city, Theor. Appl. Climatol. 84 (2006) 117–126. https://doi.org/10.1007/s00704–005–0149–9.

[82] A. Kumar, Medicinal Plants. Inernational Scientific Publishing Academy, 2010.

[83] J. Sheppard, C. Morhart, H. Spiecker, Bark surface

temperature measurements on the boles of wild cherry (Prunus avium) grown within an agroforestry system, Silva Fenn. 50 (2016). https://doi.org/10.14214/sf.1313.

[84] F. Ali-Toudert, H. Mayer, Numerical study on the effects of aspect ratio and orientation of an urban street canyon on outdoor thermal comfort in hot and dry climate, Build. Environ. 41 (2006) 94–108. https://doi.org/10.1016/j.buildenv.2005.01.013.

[85] K. Perini, A. Magliocco, Effects of vegetation, urban density, building height, and atmospheric conditions on local temperatures and thermal comfort, Urban For. Urban Green. 13 (2014) 495–506. https://doi.org/10.1016/j.ufug.2014.03.003.

[86] E.G. Mcpherson, E. Dougherty, Selecting Trees for Shade in the Southwest, J. Arboric. 15 (1989) 35–43.

[87] E.G. McPherson, Cooling Urban Heat Islands with Sustainable Landscapes, Ecol. CityPreserving Restoring Urban Biodivers. (1990) 151–171. https://doi.org/citeulike-article-id:2205597.

Appendix

Table A 1 Model parameters of MMRT model

Classes	Description	Default	Units/(type)
Geometric data	Street orientation	0-360	Radian
Computational parameters	Index of rays	-	-
	Number of rays	10,000	-
	Index of ray steps	-	-
	Number of ray steps	-	-
	Ray step size (view factor)	1	m
	Ray step size (direct shortwave radiation)	0.1	m
Radiative parameters	Albedo of walls	0.4	-
	Albedo of roofs	0.15	-
	Albedo of sidewalks	0.2	-
	Albedo of roads	0.1	-
	Albedo of trees	0.18	-
	Emissivity of walls	0.9	-
	Emissivity of roofs	0.9	-
	Emissivity of sidewalks	0.95	-
	Emissivity of roads	0.95	-
	Emissivity of trees	0.96	-

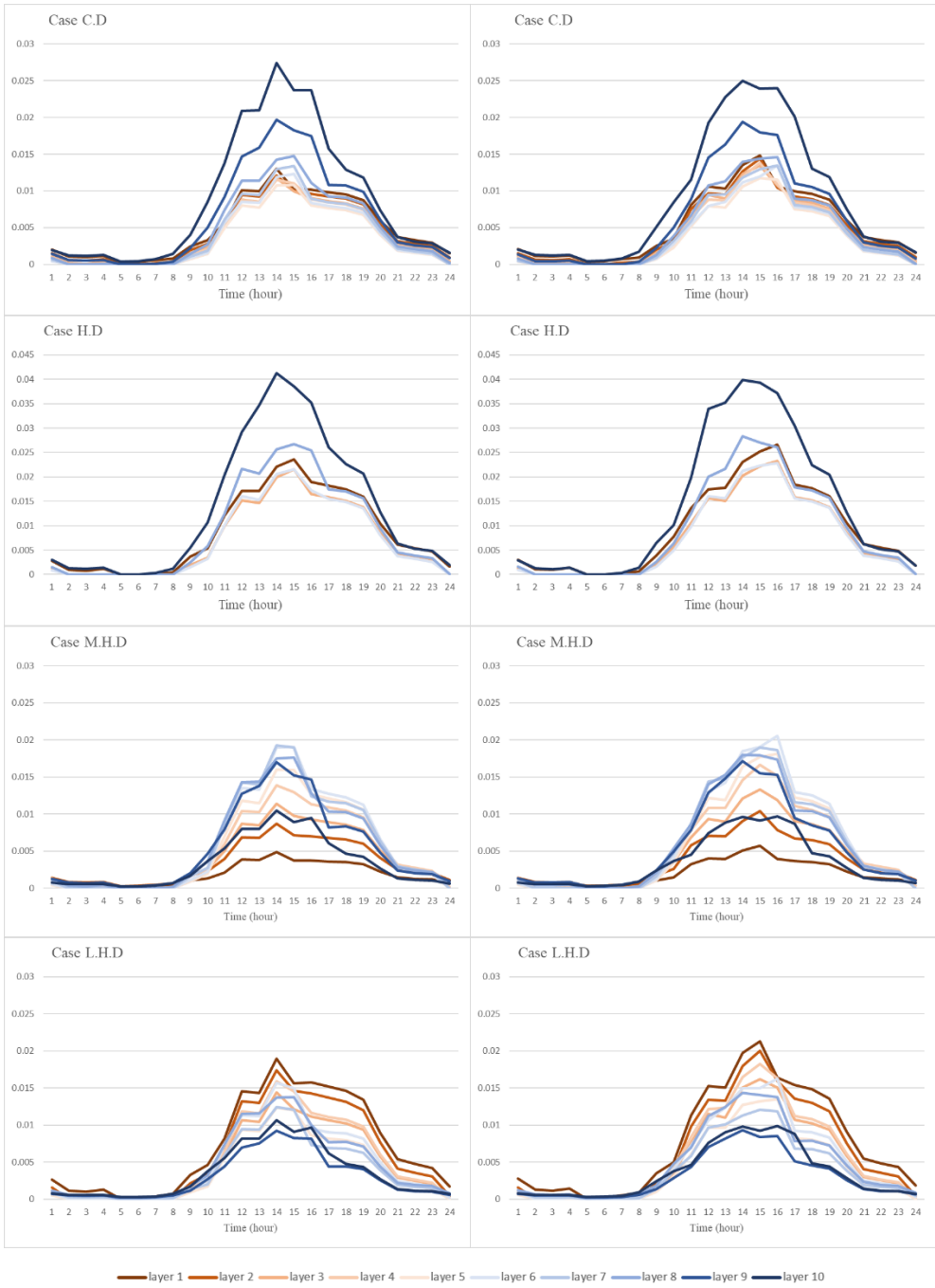

Figure A 1 Transpiration rate(g/m^2/s) of each layer surrouded by 1H buildings (Left: south tree, Right: North tree)

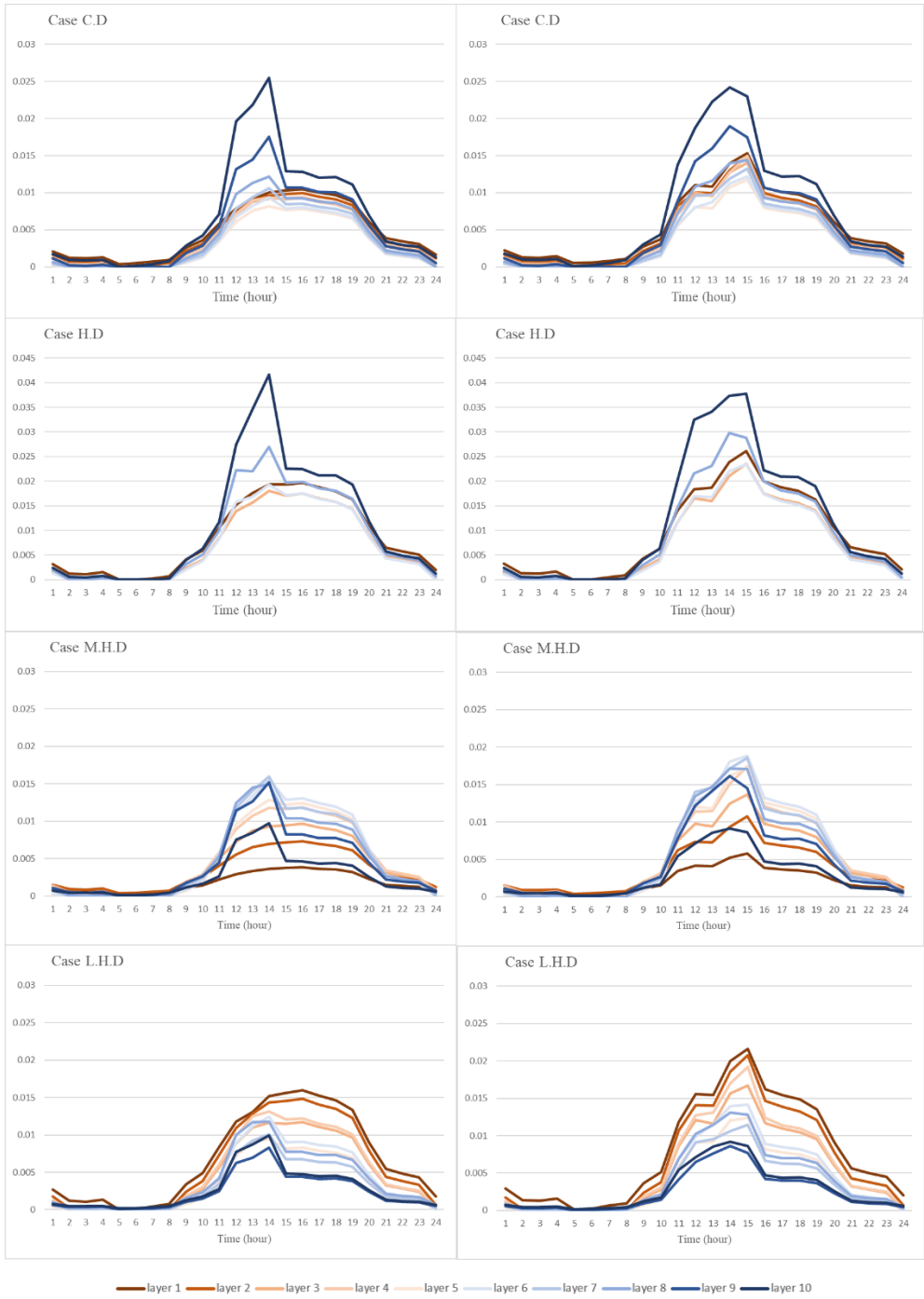

Figure A 2 Transpiration rate(g/m^2/s) of each layer surrouded by 2H buildings (Left: south tree, Right: North tree)

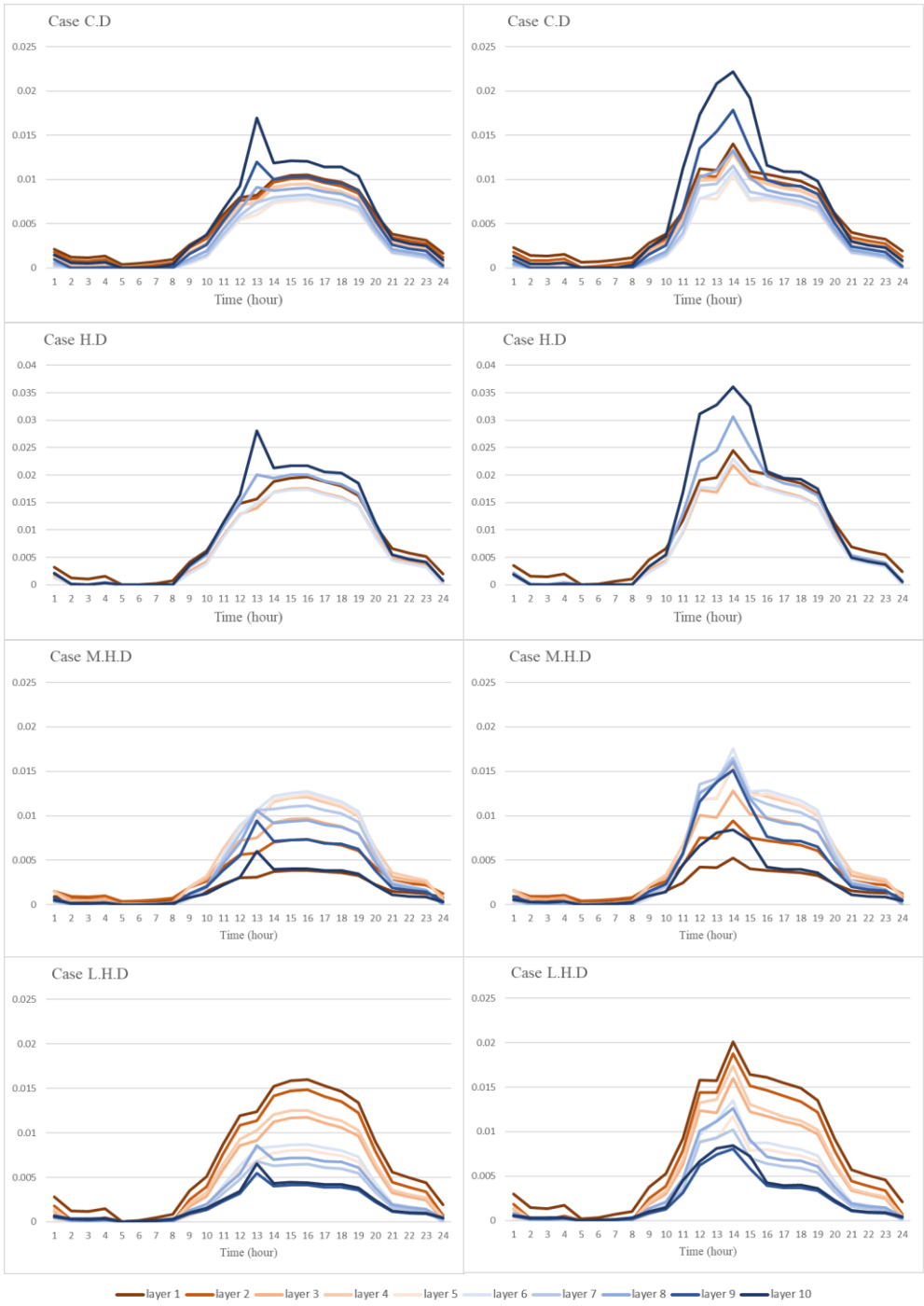

Figure A 3 Transpiration rate(g/m^2/s) of each layer surrouded by 2H buildings (Left: south tree, Right: North tree)

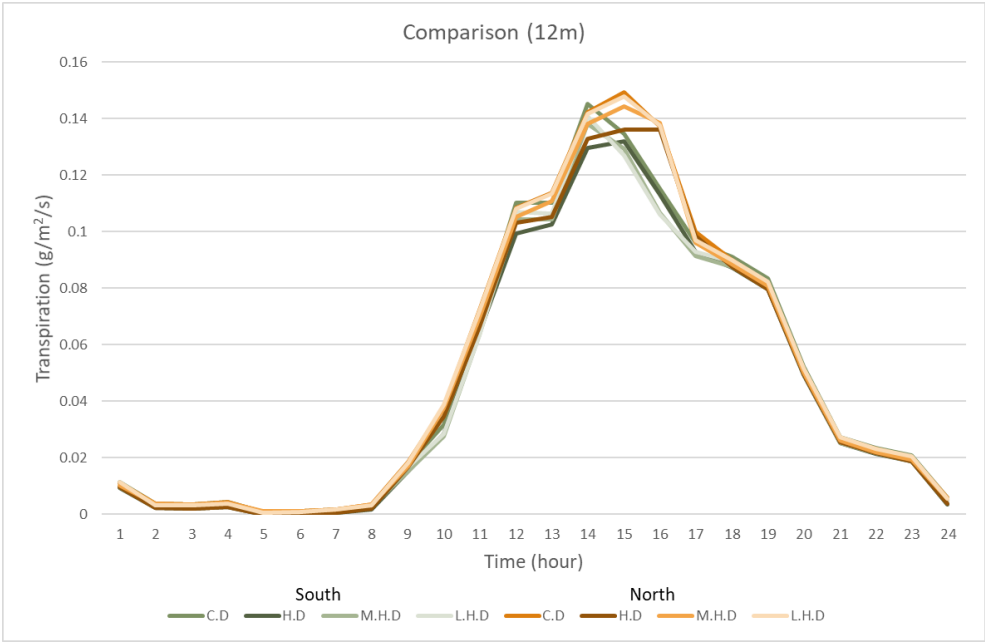

Figure A 4 Comparison of transpiration rate by changing LAD distribution & tree location (Building height: 1H)

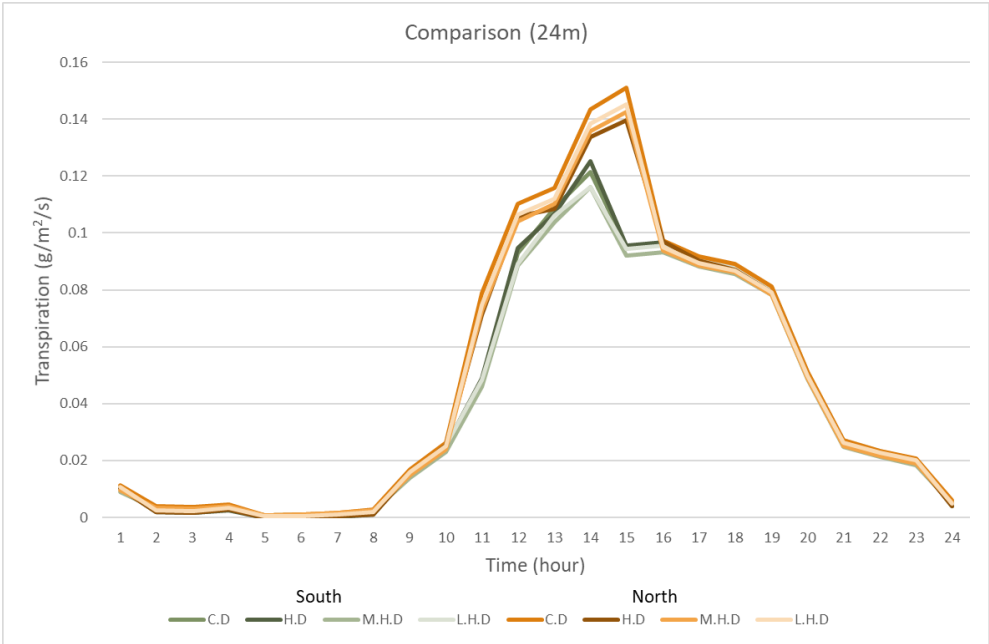

Figure A 5 Comparison of transpiration rate by changing LAD distribution & tree location (Building height: 2H)

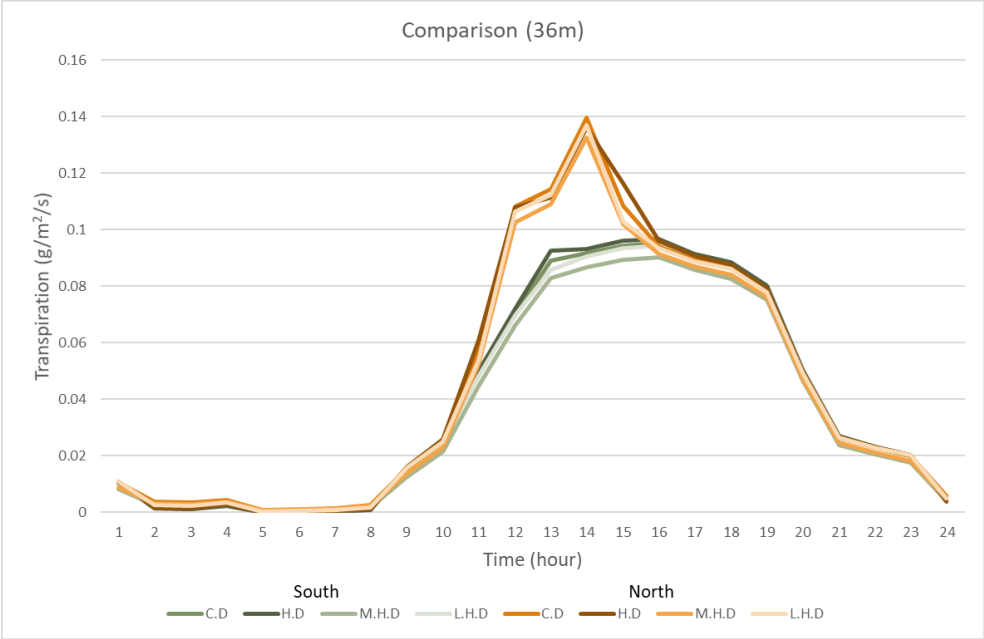

Figure A 6 Comparison of transpiration rate by changing LAD distribution & tree location (Building height: 3H)

Abstract in Korean

도시 열섬 현상이 심해짐에 따라 도시 수목의 냉각 효과가 중요해지고 있다. 수목은 복사열을 차단하거나 반사시켜 도시 표면에 도달하는 복사열을 저감시킬 수 있고, 수목의 표면온도는 아스팔트나 콘크리트 등의 불투수 표면보다 낮아 방출하는 장파 복사열을 줄일 수 있다. 또한, 수목의 증산 작용은 뿌리를 통해 흡수한 물을 잎의 기공을 통해 대기로 방출함으로써 잠열을 증가시켜 현열을 감소시킨다. 그러나, 증산량을 계산하는 대부분의 연구들은 도시 수목에 집중하지 않거나, 수목의 생리학적인 과정을 지나치게 단순화한다.

나는 수목과 건물의 수직적 구조를 고려하여 도시 수목의 증산량 산정 다층 모델을 제안한다. 이것은 광합성 활성 방사선과 잎의 표면 온도를 정확하게 모의하기 위하여 도시 캐노피 모델에서 확장되었다. 건물과 수목 환경이 증산에 주는 영향을 평가하기 위하여 건물 높이, 수목의 위치, 그리고 수목의 수직적 잎 면적 분포에 따라 달라지는 시나리오들로 증산량을 시뮬레이션하였다. 시뮬레이션은 네 가지 잎 면적 밀도(LAD) 분포를 가진 수목을 실시하였다; (1) 일정한 밀도(C.D), (2) 높은 밀도와 적은 층 (H.D), (3) 중층부에서의 높은 밀도 (M.H.D), (4) 하층부에서 높은 밀도 (L.H.D). 잎 면적 지수(LAI)와 수목의 높이는 모든 경우에서 동일하였다. 시나리오는 세 가지 건물 높이(12m, 24m, 그리고 36m)와 두 가지 수목 위치(남쪽, 북쪽)을 포함하였다. 시뮬레이션을 위해 서울에서 전후 시간에 비가 오지 않았고 높은 기온, 낮은 습도를 가진 맑은 날(2018년 8월 1일)을 선정하여 증산 작용이 크게 일어나게 하였다.

시뮬레이션 결과는 수목 구조와 주변 건물 높이에 따라 증산-효율적인 LAD 분포가 다르다는 것을 보여준다. 낮은 건물로 둘러싸인 북쪽

수목은 증산에 가장 효율적이었다. 하루 동안 수목의 증산량의 차이는 건물 높이에 따라 최대 24.1%(남쪽), 13.2%(북쪽)까지 차이가 났다. 건물 높이가 높고(3H), 낮은(1H) 시나리오에서는 LAD 분포에 따라 하루 중 수목의 증산량의 편차가 최대 8.3%(3H), 7.4(1H)였다.

이 모델은 도시의 구조나 환경에 따라 열 효율이 높은 수목 식재에 관한 가이드라인을 제공하는 데 유용한 도구가 될 수 있을 것이다. 그리고 향후 연구에서 복사열 저감 효과와 함께 분석한다면 도시 수목의 냉각 효과에 대한 보다 정확한 통찰력을 얻을 수 있을 것으로 사료된다.

Keyword : 도시 열섬, 도시 가로수, 증산 작용, 다층 모델, 도시 캐노피 모델, 냉각 효과, 잎 면적 밀도

Student Number : 2018-22915